

# Tunable-slip boundaries for coarse-grained simulations of fluid flow

J. Smiatek<sup>1</sup>, M. P. Allen<sup>2</sup>, and F. Schmid<sup>1</sup>

<sup>1</sup> Physics Faculty, Universität Bielefeld, D-33615 Bielefeld, Germany

<sup>2</sup> Department of Physics and Centre for Scientific Computing, University of Warwick, Coventry CV4 7A1, UK

the date of receipt and acceptance should be inserted later

**Abstract.** On the micro- and nanoscale, classical hydrodynamic boundary conditions such as the no-slip condition no longer apply. Instead, the flow profiles exhibit “slip” at the surface, which is characterized by a finite slip length (partial slip). We present a new, systematic way of implementing partial-slip boundary conditions with arbitrary slip length in coarse-grained computer simulations. The main idea is to represent the complex microscopic interface structure by a spatially varying effective viscous force. An analytical equation for the resulting slip length can be derived for planar and for curved surfaces. The comparison with computer simulations of a DPD (dissipative particle dynamics) fluid shows that this expression is valid from full-slip to no-slip.

**PACS.** 47.11.-j Computational methods in fluid dynamics – 47.61.-k Micro- and nano- scale flow phenomena

## 1 Introduction

In the last years much effort has been spent on the development of new microfluidic devices. Recent success in reaching the nanometer scale has stimulated rising interest in fluid mechanics on submicrometer scales. Coarse-grained computer simulations are powerful theoretical tools for investigating the dynamical properties of such confined flows. Simulation studies rely heavily on the adequate choice and implementation of the boundary conditions at the surfaces. Traditionally, solid surfaces are taken to be “no-slip” boundaries, *i.e.*, the fluid particles close to the surfaces are assumed to be at rest relative to the surface. While this can be rationalized to some extent for macroscopic (rough) surfaces [1], it has no microscopic justification. In fact, already J. C. Maxwell argued on simple kinetic grounds that there always has to be some slip at surfaces, *i.e.*, the tangential velocity does not entirely vanish at the boundaries[2,3]. In recent years, experiments have indicated that the no-slip boundary condition is indeed usually not valid on the micrometer scale[4,5]. Instead, it has to be replaced by the “partial-slip” boundary condition

$$\delta_B \partial_{\mathbf{n}} v_{\parallel} |_{\mathbf{r}_B} = v_{\parallel} |_{\mathbf{r}_B}, \quad (1)$$

where  $v_{\parallel}$  denotes the tangential component of the velocity and  $\partial_{\mathbf{n}} v_{\parallel}$  its spatial derivative normal to the surface, both evaluated at the position  $\mathbf{r}_B$  of the so-called “hydrodynamic boundary”. This boundary condition is characterized by two effective parameters, namely (i) the slip length  $\delta_B$  and (ii) the hydrodynamic boundary  $\mathbf{r}_B$ . We note that the latter does not necessarily coincide with the

physical boundary. A boundary condition of the form (1) can be formulated very generally, even in situations where the “physical boundary” is not well-defined, *e.g.*, on surfaces covered with a coating or a wetting layer. Eq. (1) has been shown to be the most general hydrodynamic boundary condition compatible with conservation laws and irreversible thermodynamics[1].

The question arises how to implement such partial-slip boundary conditions in computer simulations. Despite the experimental observation, most coarse-grained simulation models have aspired to realize no-slip boundary conditions. This task already turned out to be much more challenging than one might expect. For the dissipative particle dynamics (DPD) simulation method [6,7], several papers have been devoted specifically to the problem of reaching no-slip at the boundaries. Solid boundaries have been modeled, *e.g.*, by frozen fluid regions[6,8], or by planar walls containing one or several layers of embedded particles[9,10,11]. It is worth noting that the presence of frozen embedded particles alone does not warrant no-slip – they have to be supplemented by a bounce-back reflection law at the walls. However, these may generate artifacts in the temperature profiles[9]. Approaches to implementing arbitrary partial-slip boundary conditions in Lattice-Boltzmann have recently been proposed by Benzi *et al.* [12,13]. However, to our best knowledge, no such method has been formulated yet for coarse-grained particle simulations.

In this paper, we propose an alternative way of implementing hydrodynamic boundary conditions in general coarse-grained simulations (DPD and other). Compared to the above mentioned methods, it has several advan-

tages. (i) It does not use embedded or frozen particles; hence, it does not introduce an artificial lateral structure in the walls, and it is cheaper from a computational point of view. (ii) It does not require the unphysical bounce-back reflections and thus avoids their possible artifacts. (iii) The basic idea is very general; it can be implemented for a wide range of simulation methods in a very straightforward way. (iv) Most importantly: The method generates full-slip, partial-slip as well as no-slip boundary conditions, and it provides a model parameter  $\alpha$  with which the slip length can be tuned continuously and systematically from full-slip to no-slip. Moreover, an analytic equation can be derived, which allows to calculate the slip length to a very good approximation as a function of  $\alpha$ .

## 2 The basic idea

The hydrodynamic boundary conditions at the surface result from interactions between the fluid particles and the walls. Depending on the microscopic structure of the wall/fluid interface, these can be quite complex. In our approach, we replace the boundaries by hard planar surfaces, and the unknown atomistic forces by an effective coarse-grained friction force between the fluid particles and the walls. This leads to a dissipation of the kinetic energy and therefore to a decelerated velocity of the fluid close to the boundaries. The resulting slip length depends on the strength of the friction force. At friction force zero, one has a full-slip surface, *i.e.*, slip length infinity. With increasing friction strength, the slip length decreases.

The idea can be applied very generally. In the following, we will focus on particle-based off-lattice simulations. The friction force can then be implemented by introducing spatially varying Langevin forces acting on particles  $i$ ,

$$\mathbf{F}_i^L = \mathbf{F}_i^D + \mathbf{F}_i^R \quad (2)$$

The dissipative contribution

$$\mathbf{F}_i^D = -\gamma_L \omega_L(z_i/z_c) (\mathbf{v}_i - \mathbf{v}_{wall}) \quad (3)$$

couple to the relative velocity ( $\mathbf{v}_i - \mathbf{v}_{wall}$ ) of the particle with respect to the wall, with a locally varying viscosity  $\gamma_L \omega_L(z_i/z_c)$  that depends on the wall-particle distance  $z_i$ , with a cutoff distance  $z_c$ . The weighting function  $\omega_L(\tau)$  is positive for  $\tau < 1$  and zero for  $\tau > 1$ . Otherwise, it can be chosen freely. The prefactor  $\gamma_L$  can be used to tune the strength of the friction force and hence the value of the slip length. To preserve the global temperature  $T$  and to ensure the correct equilibrium distribution, a random force obeying the fluctuation-dissipation relation has to be added,

$$\mathbf{F}_{i,\alpha}^R = \sqrt{2\gamma_L k_B T \omega_L(z_i/z_c)} \chi_{i,\alpha} \quad (4)$$

with  $\alpha = x, y, z$ , where  $k_B$  is the Boltzmann constant and  $\chi_{i,\alpha}$  a Gaussian distributed random variable with mean zero and unit variance:  $\langle \chi_{i,\alpha} \rangle = 0$ ,  $\langle \chi_{i,\alpha} \chi_{j,\beta} \rangle = \delta_{ij} \delta_{\alpha\beta}$ . Eq. (2) can be used to model interactions with immobile walls (such as channel boundaries) as well as interactions

with surfaces of mobile and/or rotating objects (such as colloids). In the latter case, the force (2) must be balanced by a counterforce  $-\mathbf{F}_i^L$  and a countertorque  $-(\mathbf{r}_i - \mathbf{R}) \times \mathbf{F}_i^L$  acting on the object ( $\mathbf{R}$  being its center of mass).

An analytical expression for the slip length shall be derived in the next section. In short, we find that the result can be written as a function of the dimensionless parameter

$$\alpha = z_c^2 \gamma_L \rho / \eta, \quad (5)$$

where  $\rho$  is the fluid density and  $\eta$  its shear viscosity. To leading order in  $\alpha$ , the slip length is given by

$$\frac{\delta_B}{z_c} = \frac{1}{\alpha \int_0^1 d\tau \omega(\tau)} + \mathcal{O}(\alpha^0). \quad (6)$$

The sign of the next-to-leading correction is usually negative. For example, a steplike weight profile  $\omega(\tau) = 1$  for  $\tau < 1$ ,  $\omega(\tau) = 0$  otherwise, gives

$$\frac{\delta_B}{z_c} = \frac{1}{\alpha} - \frac{2}{3} - \frac{1}{45}\alpha + \dots \quad (7)$$

(cf. eq. (19) and a linear function  $\omega(\tau) = 1 - \tau$ )

$$\frac{\delta_B}{z_c} = \frac{2}{\alpha} - \frac{7}{15} - \frac{19}{1800}\alpha + \dots \quad (8)$$

(cf. eq. (20)). Hence the slip length becomes zero for an appropriate choice of  $\alpha$ , and it can be tuned to any value up to infinity (corresponding to  $\alpha = 0$ ).

## 3 Theory

The theory is based on one crucial assumption: The Navier-Stokes equations are taken to be valid on the length scale  $z_c$  of the cutoff. This assumption may seem bold, given that  $z_c$  will typically be chosen of the order of one particle diameter. However, computer simulations [14,15] have shown that the Navier-Stokes equations are valid down to surprisingly small length scales. This is also supported by our own simulations (see below).

For simplicity, we begin with discussing planar surfaces. The coordinate system is chosen such that the surface is at rest and located at  $z = 0$ . The stationary Stokes equation for our system reads

$$\eta v''(z) = \rho \gamma_L \omega_L(z/z_c) v(z) - \rho f_{ext} \quad (9)$$

with the fluid density  $\rho$  and the shear viscosity  $\eta$ . Here, we assume that the fluid viscosity does not change in the vicinity of the walls. The external force  $f_{ext}$  incorporates, *e.g.*, the effect of a pressure gradient in the direction of flow. The physical wall in our system is smooth, and we have no explicit solid/fluid wall friction. Thus the shear stress in the fluid must vanish, and the velocity field  $v(z)$  satisfies the boundary condition

$$v'(z=0) = 0. \quad (10)$$

We recall that the viscous force  $\gamma_L \omega_L(z/z_c) v(z)$  is only active within a layer of finite thickness  $z_c$ . The total friction force per surface area generated in this layer is given by

$$F/A = \rho \gamma_L \int_0^{z_c} dz \omega_L(z/z_c) v(z). \quad (11)$$

Our goal is to replace the layer by an effective boundary between a solid and an unperturbed fluid, *i.e.*, a hypothetical fluid not subjected to the additional viscous forces in the layer. The friction force per surface area,  $F/A$ , is then equal to the frictional stress on the solid, and to the shear stress on the unperturbed fluid at the position  $z = z_B$  of the boundary. This yields the effective boundary conditions

$$-F/A = \zeta_B v^{(0)}(z_B) = \eta v^{(0)'}(z_B), \quad (12)$$

where  $v^{(0)}$  is the unperturbed velocity profile, and  $\zeta_B$  the fluid-solid friction coefficient. The comparison with eq. (1) shows that the slip length can be identified with  $\delta_B = \eta/\zeta_B$ .

We first show that the hydrodynamic boundary must be identical with the physical boundary,

$$z_B = 0. \quad (13)$$

To this end, we first insert eq. (9) in eq. (11) and perform a partial integration, taking advantage of the boundary condition (10), to obtain

$$-F/A = \eta v'(z_c) + \rho f_{ext} z_c. \quad (14)$$

According to eq. (12), this must be equal to  $\eta v^{(0)'}(z_B)$ . The unperturbed velocity profile  $v^{(0)}$  solves the Stokes equation at  $\gamma_L = 0$  with the boundary conditions

$$v^{(0)}(z_c) = v(z_c); \quad v^{(0)'}(z_c) = v'(z_c). \quad (15)$$

In the planar case (9), one obtains

$$v^{(0)}(z) = v(z_c) + v'(z_c)(z - z_c) - \frac{\rho}{2\eta} f_{ext} (z - z_c)^2 \quad (16)$$

and hence

$$\eta v^{(0)'}(z_B) = \eta v'(z_c) + f_{ext} \rho (z_c - z_B). \quad (17)$$

Comparing eqs. (17) and (14) gives eq. (13).

Next we calculate the slip length. This is most conveniently done for the case  $f_{ext} = 0$ . We first integrate eq. (9) for given  $v(0) =: v_0$  and  $v'(0) = 0$  (eq. (10)) to get  $v(z_c)$  and  $v'(z_c)$ . *Via* eq. (16), we then determine the values  $v^{(0)}(z_B)$  and  $v^{(0)'}(z_B)$  of the unperturbed profile at the hydrodynamic boundary. This finally allows to calculate the slip length from

$$\delta_B = v^{(0)}(z_B)/v^{(0)'}(z_B) \quad (18)$$

(*cf.* eq. (12)). We note that all profiles scale linearly with  $v_0$ , hence the final expression for the slip length does not depend on  $v_0$  any more. More generally, the result depends only on the dimensionless quantity  $\alpha$  defined in eq. (5),

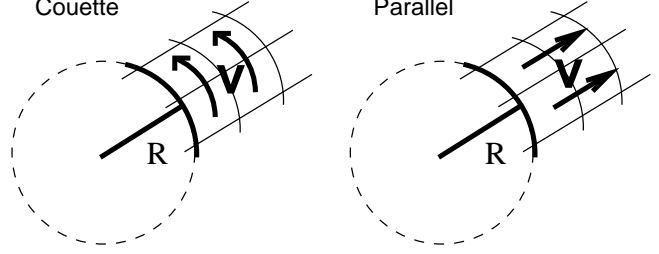


**Fig. 1.** Two types of cylindrically curved geometries. In the Couette geometry (left), the flow profile bends along the curved surface. In the parallel geometry, the fluid flows in the perpendicular direction.

in the sense that the slip length in units of  $z_c$ , *i.e.*, the quantity  $\delta_B/z_c$ , can be written as a function of  $\alpha$  only. For example, if the weight function  $\omega_L(\tau)$  is a simple step function,  $\omega_L(\tau) = 1$  for  $\tau < 1$ , the flow profile  $v(z)$  at  $z < z_c$  is a superposition of exponentials  $\exp(\pm\sqrt{\alpha}z)$ , and one obtains

$$\frac{\delta_B}{z_c} = \frac{1}{\sqrt{\alpha} \tanh(\alpha)} - 1. \quad (19)$$

If  $\omega_L(\tau)$  drops linearly to zero,  $\omega_L(\tau) = 1 - \tau$ , the profile can be written as (see appendix A)

$$\frac{\delta_B}{z_c} = -1 + \frac{1}{(3\alpha)^{1/3}} \frac{\Gamma(\frac{1}{3})}{\Gamma(\frac{2}{3})} \frac{I_{-2/3}(\frac{2\sqrt{\alpha}}{3})}{I_{2/3}(\frac{2\sqrt{\alpha}}{3})}, \quad (20)$$

where  $\Gamma$  is the Gamma-Function and  $I$  the modified Bessel function of the first kind.

The slip length can become zero (corresponding to no-slip) or even negative. The no-slip boundary condition is obtained at  $\alpha = 1.433$  for a steplike weight function, and at  $\alpha = 3.973$  for a linear weight function. Negative slip lengths are encountered at even larger  $\alpha$ . In this case, the hypothetical unperturbed profile  $v^{(0)}$  changes sign close to the boundary. We note that the true velocity profile,  $v(z)$ , never changes sign; hence our negative slip lengths do not correspond to unphysical situations.

In the regime of positive slip lengths,  $\alpha$  is small and can be used as an expansion parameter. Expanding eqs. (19) and (20) in powers of  $\alpha$  gives (7) and (8). More generally, one can derive a useful expression for arbitrary weight functions. We first note that the true velocity profile and the unperturbed profile are identical at the order  $\alpha^0$ , *i.e.*,  $v(z) = v^{(0)}(z) + \mathcal{O}(\alpha)$ . Furthermore, the derivative of the velocity profiles is of order  $\alpha$ , by virtue of eqs. (11), (12), and (17), hence one even has  $v(z) = v^{(0)}(z_B) + \mathcal{O}(\alpha)$ . Applying once more eqs. (11), (12), and (16), we obtain eq. (6). This equation allows to estimate the slip length reasonably accurately for arbitrary choices of the weight function  $\omega(\tau)$ .

The extension of the theory to curved geometries is straightforward. Here we discuss cylindrical curvature (*i.e.*, edges). One has to distinguish between curvature in the direction of flow (the ‘‘Couette’’ case) and curvature in the transverse direction (the ‘‘parallel’’ case), see Fig. 1.

The curvature is characterized by the radius  $R$  of a tangent sphere, which we take by convention to be positive at the surface of convex objects, and negative at the surface of concave objects. Details of the calculation are given in the appendix B. As in the planar case, the hydrodynamic boundary is found to be identical with the physical boundary. To leading order of  $\alpha$ , the slip length is given by

$$\frac{z_c}{\delta_B} = \frac{z_c}{R} + \alpha \int_0^1 d\tau \omega(\tau) \left(1 + \tau \frac{z_c}{R}\right)^2 + \mathcal{O}(\alpha^0). \quad (21)$$

in the Couette case, and

$$\frac{z_c}{\delta_B} = \alpha \int_0^1 d\tau \omega(\tau) \left(1 + \tau \frac{z_c}{R}\right) + \mathcal{O}(\alpha^0). \quad (22)$$

in the parallel case. In the Couette case, the inverse slip length has a contribution  $\frac{1}{R}$  of purely geometric origin. The existence of this term has been pointed out by Einzel *et al.* [1]. The remaining term can be identified with a “microscopic” inverse slip length. Both in the Couette and the parallel case, this microscopic slip length is reduced at the surface of convex objects, and enhanced at the surface of concave objects.

## 4 Comparison with computer simulations

To test the method and the theory, we have carried out dissipative particle dynamics[6,7] (DPD) simulations of fluids confined in a parallel slit. The fluid particles interact with purely dissipative DPD forces of range  $\sigma$  [7]. They have no conservative interactions with each other, their static equilibrium structure is thus that of an ideal gas. They are confined into the slit by two parallel walls, with which they interact *via* a Weeks-Chandler-Andersen potential [16] with characteristic length  $\sigma$ ; alternatively, one can use hard reflecting walls. In the vicinity of the walls, up to the cutoff distance  $z_c$ , the particles experience a wall friction force of the form (2) with a linear weight function,  $\omega_L(\tau) = 1 - \tau$ . The choice of the weight function is in fact completely arbitrary. It was motivated by the fact that the DPD weight factors for intermolecular dissipative interactions are also usually chosen linear for reasons of computational efficiency. The natural units of the simulation are the length unit  $\sigma$ , the thermal energy  $k_B T =: \epsilon$ , and the mass of the particles  $m$ . In these units, the cutoff at the walls was chosen  $z_c = \sigma$ , and the time step  $\delta t = 0.01 \sigma \sqrt{m/\epsilon}$ . Periodic boundary conditions were applied in the slit plane. All simulations were carried out with extensions of the simulation package ESPResSo[17,18,19].

We have simulated both planar Couette and planar Poiseuille flow[20]. In the first case, one of the walls moves at constant speed relative to the other. In the second case, the effect of the pressure gradient is mimicked by a constant force acting on all particles in the slit. Fig. 2 shows two examples of flow profiles. Sufficiently far from the walls, the classical parabolic Poiseuille flow and linear Couette flow profiles are nicely recovered.

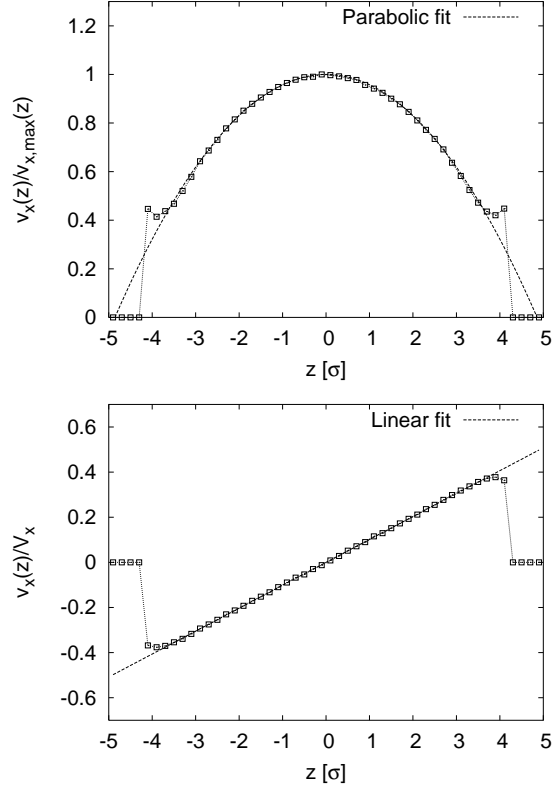


**Fig. 2.** Normalised plane Poiseuille flow (top) and plane Couette flow (bottom) for DPD fluids ( $\gamma_{DPD} = 5\sqrt{m\epsilon}/\sigma$ ) with number density  $\rho = 3.75\sigma^{-3}$ . The parameters of the surface friction force are  $\gamma_L = 1.0\sqrt{m\epsilon}/\sigma$ ,  $z_c = \sigma$ . The dashed lines show fits to the theoretical profiles.

The combined results from the Poiseuille and Couette fits allows to calculate the slip length and the position of the hydrodynamic boundary independently: We determine the distance  $P$  between the two points where the extrapolated Poiseuille parabola vanishes, and the distance  $C$  between the two points where the extrapolated Couette line reaches the velocities of the two walls. The slip length is then given by

$$\delta_B^2 = (C^2 - P^2)/4, \quad (23)$$

and the hydrodynamic boundary is located at the distance

$$z_B = \delta_B - (C - L)/2. \quad (24)$$

from the physical boundary, where  $L$  is the distance between the two physical walls. We note that both  $C$  and  $P$  enter the expression for the slip length, hence both the Poiseuille and the Couette profile have to be simulated. This is because we do not make any assumptions regarding the hydrodynamic boundary. If its position is unknown, two types of profiles have to be measured in order to determine the two parameters  $z_B$  and  $\delta_B$ . This fact is not always appreciated in the literature.

We have determined the hydrodynamic boundary and the slip length for the range of parameters  $\gamma_L = (0.1 - 5) \sqrt{m\epsilon}/\sigma$  (the friction at the wall),  $\rho = (3.75-12.5) \sigma^{-3}$

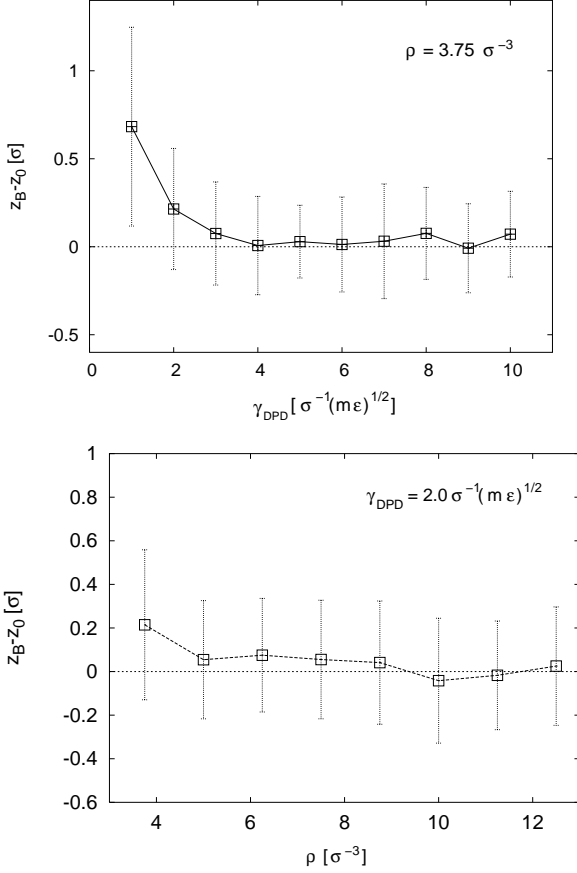


**Fig. 3.** Position of the hydrodynamic boundaries for varying  $\gamma_{DPD}$  and fixed number density  $\rho = 3.75\sigma^{-3}$  (top) and for varying rho and fixed  $\gamma_{DPD} = 2\sqrt{m\epsilon}/\sigma$  (bottom). The result does not depend on the value of the surface friction  $\gamma_L$ . The data shown here are averaged over all  $\gamma_L$ .

(the number density of fluid particles), and  $\gamma_{DPD} = (1-10)\sqrt{m\epsilon}/\sigma$  (the friction coefficient of the DPD forces). The results are summarized in the figures 3 and 4. The theory predicts that the hydrodynamic boundary is identical with the physical boundary, eq. (13). This was found to be correct for most systems. Significant deviations were only encountered at small DPD-friction  $\gamma_{DPD}$  (fig. 3). Fig. 4 shows the results for the slip length as a function of the dimensionless parameter  $\alpha = \gamma_L \rho z_c^2 / \eta$ . The shear viscosity  $\eta$  of the fluids was determined from the Poiseuille fits[21]. The numerical results for the slip length compare very favorably with the theoretical prediction of eq. (8), except in the regime where the hydrodynamic boundary also deviates from its theoretical position, *i.e.*, at small DPD-friction  $\gamma_{DPD}$ . Even in this regime, the method can still be used to produce partial slip. A wide range of slip lengths has been realized. The inset of Fig. 4 illustrates that the no-slip regime can also be reached very naturally.

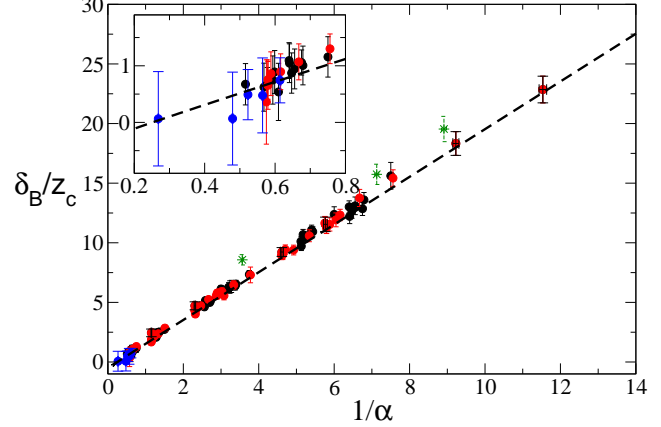


**Fig. 4.** Slip length  $\delta_B$  in units of  $z_c$  vs.  $\alpha$  for varying values of the parameter triplet  $(\rho, \gamma_{DPD}, \gamma_L)$  (in units of  $\sigma^{-3}$  or  $\sqrt{m\epsilon}/\sigma$ , respectively). Black: series with  $\rho$  fixed: (3.75, 2-10, 0.1-1). Red: series with  $\gamma_{DPD}$  fixed: (3.75-12.5, 2, 0.1-1). Blue: selected triplet values: (6.35,5,1), (5,5,1), (11.25,2,1.1), (11.25,2,1.2), (3.75,10,2.5). Green star symbols: series corresponding to the point in fig. 3, where the position of the hydrodynamic boundary deviates from theoretical expectation: (3.75,1,0.1-1). Dashed black line: Theoretical prediction of eq. (20). The inset shows a blowup of the same data.

## 5 Summary

We have presented a method that allows to implement arbitrary hydrodynamic boundary conditions in coarse-grained simulations. We have illustrated and tested this method with DPD simulations; however it can be applied much more generally. The main idea is to introduce an effective surface friction force, complemented by an appropriate thermostat. This idea can also be implemented, *e.g.*, in stochastic rotation dynamics simulations or in Lattice Boltzmann simulations. The strength of the friction force effectively determines the slip length. We have shown that our method allows one to tune the slip length systematically from full-slip to no-slip. Furthermore, we have derived an analytical equation for the slip length as a function of the strength of the friction force and the shear viscosity of the fluid.

An alternative force-driven method to control the slip length on surfaces has recently been proposed for the Lattice Boltzmann simulation method by Benzi et al[12]. In this work, conservative forces are introduced that deplete the fluid density at the surface, which leads to partial slip – a physical effect. In contrast, the dissipative forces in our method mimic directly the effective friction between the surface and the bulk fluid. While the method does thus not contribute to a microscopic understanding of the slip at surfaces, it does offer a way to model the essential wall properties, from the hydrodynamics point of view, and to absorb the complex wall structure into a well-defined coarse-grained parameter set[13]. The method can be implemented easily, it generates the partial-slip boundary conditions for microfluidic simulations that are observed in experiments. Curvature can be introduced in a straightforward manner, the effect of curvature on the slip length

in the model can be calculated analytically, and corrected by an easy change of local friction if necessary. Hence the method is suitable to study complex geometries and/or objects, such as structured channels, channels with objects, or rotating nanoparticles in flow.

The only obvious restriction is that the characteristic length scale of the structures has to be larger than the length scale  $z_c$  on which the friction force is applied. In future work, it will be interesting to determine the minimal lateral length scale that the method can handle, *e.g.*, by studying surfaces with mixed boundary conditions. For example, analytical results are available for the macroscopic effective slip length on surfaces covered by stripes with alternating full-slip and no-slip boundary conditions[22,23], and the Stokes equation has also been solved numerically for more general mixed surfaces[24,25]. This will be a good starting point for a systematic study. Furthermore, we plan to apply our method to the simulation of electrolyte flow to assess the influence of partial-slip boundary conditions on electroosmotic flow[26].

We thank Burkhard Dünweg, Christian Holm and Ulf D. Schiller for nice and fruitful discussions. This work was funded by the Volkswagen Stiftung. The visit of MPA to Bielefeld was supported by the Alexander von Humboldt foundation.

## 6 Appendices

### A: Slip length for linear weight function

The program for calculating the slip length (Eq. (18)) can easily be carried out numerically for arbitrary weight functions  $\omega(\tau)$ . For some simple choices of the weight function, analytical results can also be obtained. To illustrate the approach, we sketch the calculation leading to Eq. (20), the expression for the slip length for a linear weight function  $\omega(\tau) = 1 - \tau$ .

In the absence of an external force ( $f_{ext} = 0$ ), the general solution of Eq. (9) for a linear weight function reads

$$v(z) = A \text{Ai}(c(1 - z/z_c)) + B \text{Bi}(c(1 - z/z_c)) \quad (\text{A.2})$$

with  $c = -(-\alpha)^{1/3}$ , where Ai and Bi are the Airy functions and  $\alpha$  has been defined in Eq. (5). The boundary conditions  $v(0) = v_0$ ,  $v'(0) = 0$  determine the coefficients

$$\begin{aligned} A &= v_0 \text{Ai}'(c) / (\text{Ai}'(c)\text{Bi}(c) - \text{Ai}(c)\text{Bi}'(c)) \\ B &= v_0 \text{Bi}'(c) / (\text{Ai}'(c)\text{Bi}(c) - \text{Ai}(c)\text{Bi}'(c)). \end{aligned}$$

The unperturbed profile is linear,  $v^{(0)}(z) = v(z_c) + v'(z_c)(z - z_c)$ , and the hydrodynamic boundary is located at  $z_B = 0$  according to Eq. (13), hence the equation (18) for the slip length can be written as

$$\frac{\delta_B}{z_c} = \frac{v(z_c)}{z_c v'(z_c)} - 1. \quad (\text{A.3})$$

Inserting this in Eqs. (A.2) with (A.3) and (A.3) and using the identities  $\text{Ai}(0) = 1/(3^{2/3}\Gamma(\frac{2}{3}))$ ,  $\text{Ai}'(0) = -1/(3^{1/3}\Gamma(\frac{1}{3}))$ ,

$\text{Bi}(0) = \sqrt{3}\text{Ai}(0)$ , and  $\text{Bi}'(0) = -\sqrt{3}\text{Ai}'(0)$ , where  $\Gamma$  is the Euler gamma function, one obtains

$$\frac{\delta_B}{z_c} = -1 - \frac{1}{3^{1/3}c} \frac{\Gamma(\frac{1}{3})}{\Gamma(\frac{2}{3})} \frac{\text{Ai}'(c)\sqrt{3} - \text{Bi}'(c)}{\text{Ai}'(c)\sqrt{3} + \text{Bi}'(c)}. \quad (\text{A.4})$$

To get rid of the complex argument  $c$ , we use the series expansion of the Airy functions[27]. The functions of interest for us can be written as  $\text{Ai}'(z)\sqrt{3} = I_1 - I_2$  and  $\text{Bi}'(z) = I_1 + I_2$  with

$$\begin{aligned} I_1 &= \frac{z^2}{3} \sum_k \frac{1}{3^{1/6} \Gamma(k + 5/3) k!} \left(\frac{z^3}{9}\right)^k \\ I_2 &= 3^{1/6} \sum_k \frac{1}{\Gamma(k + 1/3) k!} \left(\frac{z^3}{9}\right)^k. \end{aligned}$$

Comparing this with the series representation of the modified Bessel function of the first kind,

$$I_\nu(z) = \left(\frac{z}{2}\right)^\nu \sum_k \frac{1}{\Gamma(k + \nu + 1) k!} \left(\frac{z}{2}\right)^{2k}, \quad (\text{A.5})$$

one easily verifies the identities

$$I_1 = -\frac{\alpha^{1/3}}{\sqrt{3}} I_{-2/3}\left(\frac{2\sqrt{\alpha}}{3}\right) \quad \text{and} \quad I_2 = \frac{\alpha^{2/3}}{\sqrt{3}c} I_{2/3}\left(\frac{2\sqrt{\alpha}}{3}\right).$$

Inserting this into Eq. (A.4) gives Eq. (20).

### B: Curved boundaries

The strategy for calculating the slip length and the hydrodynamic boundary position at curved surfaces is perfectly analogous to that sketched in the main text for the planar geometry. We begin with noting that the expression for the total friction force per surface area, eq. (11), acquires an additional geometric factor at curved surfaces,

$$F/A = \rho \gamma_L \int_R^{R+z_c} dr \omega_L((r - R)/z_c) v(r) \frac{r}{r_B}, \quad (\text{A.6})$$

which accounts for the fact that the viscous layer is stretched or compressed in the presence of curvature. Here,  $R$  is the radius of curvature,  $r$  the distance from the center of the tangent sphere, and  $r_B$  the position of the hydrodynamic boundary. Furthermore, the Stokes equation, (9), and the boundary conditions, (10) and (12) have to be replaced by the appropriate cylindrical versions.

We first discuss the Couette case. The Stokes equation for this geometry reads

$$\eta \partial_r \frac{1}{r} \partial_r r v(r) = \rho \gamma_L \omega((r - R)/z_c) v(r) - \rho f_{ext}, \quad (\text{A.7})$$

The unperturbed solution of this equation for  $\gamma_L = 0$  and fixed  $v(r_c) = v_c$ ,  $v'(r_c) = v'_c$  is given by

$$v^{(0)}(r) = \frac{1}{2} \left[ \frac{r}{r_c} (v_c + v'_c r_c + \tilde{f}) + \frac{r_c}{r} (v_c - v'_c r_c - \frac{\tilde{f}}{3}) - \frac{\tilde{f}}{3} \left(\frac{r}{r_c}\right)^2 \right] \quad (\text{A.8})$$

with  $\tilde{f} = \rho f_{ext} r_c^2 / \eta$ . In the absence of an external force,  $\tilde{f} = 0$ , one recovers the well-known profile of cylindrical Couette flow. The appropriate expressions for the fluid shear stress also differ from those in the planar case, and Eqs. (10) and (12) have to be replaced by[1]

$$(\partial_r v - v/r)|_{r=R} = 0, \quad (\text{A.9})$$

$$-F/A = \zeta_B v^{(0)}(r)|_{r=r_B} = \eta(\partial_r v^{(0)} - v^{(0)}/r)|_{r=r_B}. \quad (\text{A.10})$$

Comparing eq. (A.10) with eq. (1), one immediately obtains  $\delta_B^{-1} = \delta_0^{-1} + r_B^{-1}$  with  $\delta_0^{-1} = \zeta_B/\eta$ , where  $r_B^{-1}$  is a geometric contribution, and  $\delta_0^{-1}$  incorporates the specific effect of the surface structure. Comparing with eq. (A.6), one gets

$$\frac{z_c}{\delta_0} = \alpha \int_0^1 d\tau \omega_L(\tau) \frac{v(R + \tau z_c)}{v^{(0)}(r_B)} \frac{R + \tau z_c}{r_B}. \quad (\text{A.11})$$

For fixed  $v(R + z_c) = v_c$ ,  $v'(R + z_c) = v'_c$ , the actual profile  $v(r)$  is identical with the unperturbed profile  $v^{(0)}(r)$  of eq. (A.8) at leading order of  $\alpha$ . Inserting this in eq. (A.11) and using  $r_B = R$ , we finally recover eq. (21). To establish the identity  $r_B = R$ , we require again that the total friction force as given by eq. (A.6) is identical with the hypothetical shear stress on the unperturbed fluid, eq. (A.10). Inserting (A.7) in (A.6), carrying out a few partial integrations, using (A.9), and finally replacing once more  $v(r)$  by  $v^{(0)}(r)$  at order  $\alpha$ , we obtain

$$-\frac{F}{A} = \frac{\eta}{r_B} \frac{r_c}{R} \left\{ -v_c + v'_c r_c + \frac{\tilde{f}}{3} \left( 1 + \left( \frac{R}{r_c} \right)^3 \right) \right\} + \mathcal{O}(\alpha). \quad (\text{A.12})$$

Comparing this with eq. (A.10), after inserting (A.8), we find that  $r_B$  must be equal to the surface position  $R$  at the leading order of  $\alpha$ .

The parallel case is even simpler. The appropriate Stokes equation reads

$$\frac{1}{r} \partial_r r \partial_r v(r) = \rho \gamma_L \omega((r - R)/z_c) v(r) - \rho f_{ext}. \quad (\text{A.13})$$

In the unperturbed case  $\gamma_L = 0$ , this is solved by

$$v^{(0)}(r) = v_c + (v'_c r_c + \frac{\tilde{f}}{2}) \ln\left(\frac{r}{r_c}\right) + \frac{\tilde{f}}{4} \left( 1 - \left( \frac{r}{r_c} \right)^2 \right) \quad (\text{A.14})$$

with  $v_c := v(r_c)$ ,  $v'_c := v'(r_c)$ , and  $\tilde{f} = \rho f_{ext} r_c^2 / \eta$  as before. The expressions for the fluid shear stress are similar to those in the planar case,

$$\partial_r v|_{r=R} = 0, \quad (\text{A.15})$$

$$-F/A = \zeta_B v^{(0)}(r)|_{r=r_B} = \eta(\partial_r v^{(0)} - v^{(0)}/r)|_{r=r_B}. \quad (\text{A.16})$$

Proceeding as before, we find that  $r_B = R$  is fulfilled exactly, and we recover eq. (22).

## References

1. Einzel D., Panzer P., and Liu M., Phys. Rev. Lett. **64**, (1990) 2269.
2. Maxwell J. C., Philos. Trans. Soc. London **170**, (1867) 231.
3. Kennard E. H., *Kinetic theory of gases* (McGraw-Hill, New York, 1938).
4. Pit R., Hervet H., and Leger L., Phys. Rev. Lett. **85**, (2000) 980.
5. Neto C., Evans D. R., Bonaccorso E., Butt H.-J., and Craig V. S. J., Rep. Prog. Phys. **68**, (2005) 2859.
6. Hoogerbrugge P. J. and Koelman J. M., Europhys. Lett. **19**, (1992) 155.
7. Español P. and Warren P., Europhys. Lett. **30**, (1995) 191.
8. Boek E., Coveney P., Lekkerkerker H., and van der Schoot P., Phys. Rev.E **55**, (1997) 3124.
9. Revenga M., Zuniga I., and Español P., Comp. Phys. Comm. **121-122**, (1999) 309.
10. Duong-Hong D., Phan-Thien N., and Fan X. J., Computational mechanics **35**, (2004) 24.
11. Pivkin I. V. and Karniadakis G. E., J. Comput. Phys. **207**, (2005) 114.
12. Benzi R., Biferale L., Sbragaglia M., Succi S., and Toschi F., Europhys. Lett. **74**, (2006) 651.
13. Benzi R., Biferale L., Sbragaglia M., Succi S., and Toschi F., J. Fluid Mech. **548**, (2006) 257.
14. Alder B. J. and Wainwright T. E., Phys. Rev. A **1**, (1970) 18.
15. Dünweg B. and Kremer K., J. Chem. Phys. **99**, (1993) 6983.
16. Weeks J. D., Chandler D., and Andersen H. C., J. Chem. Phys. **54**, (1971) 5237.
17. ESPResSo-Homepage, <http://www.espresso.mpg.de>.
18. Arnold A., Mann B. A., Limbach H.-J. and Holm C., *GWDG-Bericht: Forschung und wissenschaftliches Rechnen 2003* Vol. 63, Kremer K. Macho V. Eds. (Gesellschaft für wissenschaftliche Datenverarbeitung mbh, Göttingen, Germany, 2004), pp. 43 ff.
19. Limbach H.-J., Arnold A., Mann B. A., and Holm C., Comp. Phys. Comm. **174**, (2006) 704.
20. Lu P.-C., *Introduction to the mechanics of viscous fluids* (Holt, Rinehart and Winston Inc., New York 1973).
21. Backer J. A., Lowe C. P., Hoefsloot H. C. J., and Iedema P. D., J. Chem. Phys. **122**, (2005) 154503.
22. Philip J. R., J. Appl. Math. Phys. (ZAMP) **23**, (1972) 353.
23. Lauga E. and Stone H.A., J. Fluid Mech. **489**, (2003) 55.
24. Cottin-Bizonne C., Barentin C., Charlaix E., Bocquet L., and Barrat J.-L., Eur. Phys. J E **15**, (2004) 427.
25. Priezjev N.V., Darhuber A.A., and Troian S.M., Phys. Rev. E. **71**, (2005) 041608.
26. Smiatek J. et al., Poster presented at the International Soft Matter Conference, Aachen, October 2007.
27. See, e.g., [functions.wolfram.com](http://functions.wolfram.com).